# THE EFFECT OF INCLUSIONS ON THE ENVIRONMENTALLY ACCELERATED CYCLIC CRACK GROWTH OF REACTOR PRESSURE VESSEL STEELS IN SIMULATED LWR ENVIRONMENTS

K. Törrönen*, T. Saario*, H. Hänninen*, M. Kemppainen**, and S. Salonen*

The presence of reactor water is known to accelerate the cyclic crack growth of ferritic pressure vessel steels. Recently a dependence of the acceleration on the sulfur content of the steel has been observed. A series of tests is described which indicates that it is the size, shape and distribution of manganese sulfide inclusions rather than the sulfur content per se which have the strongest influence on the treshold and magnitude of the environmental acceleration. Small size and round shape of the inclusions seem to greatly reduce environmental influence on cyclic crack growth. Reasons for this observation are discussed based on postulated micro-mechanisms of environmentally accelerated crack growth.

## INTRODUCTION

Recent years have witnessed a significant increase in the amount of research and published data on fatigue crack growth for pressure vessel and piping materials in simulated light water reactor environments. There is a large number of mechanical (frequency, load ratio and waveform), environmental ($O_2$-content, potential and temperature) and material related (product form, composition, inclusion morphology and irradiation) effects which are being carefully investigated on a macroscopic scale. However, micromechanistic understanding of corrosion fatigue is far from complete, although many theories have been presented (Tomkins (1), Cullen et al. (2), Bamford and Moon (3), Törrönen et al. (4), Scott and Truswell (5), Hänninen et al. (6)).

This paper describes some new attempts to gain further understanding of these micromechanisms, and presents an interpretation of the experimental data based on a hydrogen-induced cracking model. The role of inclusions is of special concern.

## EXPERIMENTAL METHODS

Two pressure vessel steels were tested, i.e. A533B Cl 1 and CrMoV steel. Compact tension specimens (1TCT) in the T-L and T-S orientation, respectively, were used. The testing was conducted in pressurized high-temperature (288°C) low-oxygen (less than 100 ppb) high purity or simulated PWR water. 17 mHz (1 cpm) sinewave loading and load ratio of R = 0.2 were utilized. More details of the testing procedure and materials are given elsewhere (5, 6).

*Metals Laboratory and **Metallurgy Laboratory,
Technical Research Centre of Finland (VTT)

The main part of the experimental work presented here, however, consisted of fractographic analysis of the fracture surfaces and detailed inclusion size, morphology and distribution analysis in 3 dimensions.

## RESULTS

### Cyclic crack growth

An example of the cyclic crack growth rates as a function of the applied cyclic stress intensity for the two steels is shown in Fig. 1. Similar results were obtained in other tests at VTT and at other laboratories in the ICCGR round robin testing (Jones (7)). The presented fractographic analysis is based on the data shown in Fig. 1.

It has been shown formerly that the fatigue crack growth rates are connected to sulfur contents of the test materials (Amzallag and Bernard (8), Bamford and Ceschini (9)) lower sulfur contents result in a smaller environmental effect. The two studied materials were chosen for this mechanistic study since they have almost the same sulfur content but they have marked differences in MnS inclusion morphology and distribution (Fig. 2), and a very different da/dN versus $\Delta K$ relationship (Fig. 1). It is proposed that these differences in MnS inclusion morphology and distribution result in large variations in cyclic crack propagation rates. The following fractographic study will be based on this hypothesis. Important other test variables like waveform, frequency, load ratio and dissolved oxygen content, which have or might have an influence on the observed crack growth rate and consequently also on the mechanism of cracking are discussed elsewhere (4, 6).

### Fractography

The fractographic examination of corrosion fatigue specimens revealed principally three different fracture morphologies which are transgranular, ductile striations, transgranular, "brittle" striations, and striationless, cleavage-like fracture. A detailed definition for these can be found e.g. in reference (6).

The macroscopic and also microscopic fracture appearances are always similar when environmentally enhanced crack growth rates are observed (Torronen and Kemppainen (10)). Thus, there are no fractographic differences between tests in different conditions ($O_2$-content, flow rate, potential etc.). Always when environmental acceleration is observed brittle features can be seen on the fracture surface.

A fairly dense distribution of elongated MnS inclusions was evident whenever the fracture mode had brittle features. A typical feature was that a group of inclusions had generated a brittle mode of crack growth, which spread like a fan over the remaining part of the fracture path (see Fig. 5). However, this was evident only in A533B steel. On both sides of the macroscopic brittle fracture mode area, typical ductile striations could be seen throughout the fracture path. A considerably smaller amount of inclusions was found in these ductile areas. However, sometimes brittle features were also seen on the fracture surface in connection with these inclusions, although usually no change in fracture surface morphology was observed. In the CrMoV steel specimen no similar fan-shaped areas could be observed. This is thought to be due to the fact that in this steel the inclusions are small, round and more evenly distributed (see Fig. 2).

The inclusions are dissolved during the testing leaving only empty sites. However, near to the crack tip partly dissolved MnS inclusions can be observed and next to the crack tip unchanged, exposed inclusions are present. Thus, the dissolution of MnS inclusions is a time-dependent process.

Another typical feature in the fracture surface morphology is the terraced appearance caused by elongated MnS inclusions located at different levels from the main crack path (Fig. 6). These terraces are coalesced to the main fracture surface by a shear mechanism. The morphology of these terraces indicates that inclusions in the crack tip stress field can initiate cracking ahead of the main crack.

A connection between the local density of MnS inclusions and the "brittle" type of fracture surface is clear, and considerably fewer inclusions were seen on the ductile striated fracture surface. Sometimes in this case small "brittle" regions were associated with the inclusions, but not always, in A533B steel. In the CrMoV steel only ductile striations were observed and the "brittle" areas around inclusions were absent.

Inclusions seem to be capable of producing "brittle" cracking around them ahead of the main crack tip. Fig. 7 shows an example of "brittle" cracking (C) (differs from mechanical cleavage fracture (B)) around an inclusion (D) ahead of the final crack tip in the A533B steel specimen. The corrosion fatigue fracture surface is denoted by A. The distance of the inclusion from the crack tip is about 0.15 mm, which is in the area of maximum triaxial stress in front of the crack at this particular K-level.

## INCLUSION ANALYSES

The inclusion distributions of the two steels studied in this work were measured on all the three main planes, L, T and S, respective to the hot working directions. The MnS-inclusion size distributions for the plane T, which also was the plane of the corrosion fatigue crack propagation, are shown in Fig. 2. Obviously, the fraction of large (> 5 μm) inclusions is noticeably greater for the A533B-steel. The average size of the MnS-inclusions was 3.7 μm and 7.4 μm for the CrMoV-steel and the A533B-steel, respectively.

It was also found that mainly the large inclusions were highly elongated, and that in the CrMoV-steel these elongated MnS-inclusions were almost non-existent. The average nearest neighbour distances calculated from the measured area densities of inclusions were, for the plane T, about 310 μm and 170 μm for the A533B- and CrMoV-steels, respectively. The area fraction of MnS-inclusions was almost the same in both steels, which is in accord with the almost equal sulfur contents of the two steels (about 0.014 percent).

## DISCUSSION

Two basic mechanisms, dissolution-controlled and hydrogen-induced cracking, have generally been proposed to explain environmentally enhanced crack growth in simulated PWR and BWR environments (1-6). In the former process the crack propagation is controlled by anodic dissolution of the metal at the crack tip, whereas in the latter process the mechanical separation at the crack tip is facilitated by hydrogen embrittlement. Both favoured mechanisms for crack propagation depend on the same rate-determining parameters, which makes it

difficult to differentiate experimentally between these mechanisms (5). The present authors favour the latter as the main crack propagation mechanism. Our opinion is based primarily on the fractographic evidence published earlier (2, 3, 4, 6, 10) and found during this work. The most important common factors supporting the hydrogen-induced crack propagation mechanism in corrosion fatigue are brittle fracture surface morphology ("brittle" striations and cleavage-like fracture) and the role of manganese sulfide inclusions which act as hydrogen traps and seem to localize cracking to themselves. Subsequent dissolution of the MnS inclusions changes the crack tip electrochemistry and this further enhances hydrogen absorption (6).

The hydrogen-induced cracking mechanism is outlined in Fig. 4. It is further evaluated and discussed elsewhere (6).

Nakai et al. (11) have shown that hydrogen induced cracking in linepipe steels tested in $H_2S$ saturated synthetic sea water is controlled by inclusion morphology. According to their results, hydrogen induced cracking was initiated at highly elongated MnS-inclusions. They also showed, that when inclusion morphology was controlled either by rare earth metal or Ca-additions, no hydrogen induced cracks were found.

Our results on the difference between the cyclic crack growth rates (Fig. 1) and the accompanying differences in the inclusion distributions (Fig. 2) suggest that the environmental enhancement of the cyclic crack growth rate in PWR environment is also, at least partially, controlled by the MnS-inclusion morphology. Our view is that hydrogen entering the metal lattice is strongly trapped at the MnS-inclusions. The elongated inclusions, acting like microcracks, produce an intense stress-strain-distribution around themselves as they are enveloped by the plastic zone moving ahead of the fatigue crack tip. Trapped hydrogen and the microcrack-type behaviour of the elongated inclusions together with the high tensile stresses ahead of the fatigue crack tip trigger the hydrogen induced cracking found around inclusions. The beneficial aspect of spherical inclusions is in the reduction of the microcrack-type behaviour.

If we accept the above mentioned view of the process, we must also expect that the treshold $K_{max}$-value, at which the environmental enhancement quite promtly appears, corresponds to some critical size of the plastic zone, which critical value again is controlled by the density of elongated MnS-inclusions. Taking $K_{max}$=28 MPa$\sqrt{m}$ (Tomkins and Scott (12)) and using the equations (see Fig. 3) for the plastic zone size given by Knott (13), we obtain the results shown in Fig. 3. As we see, the extent of the plastic zone in the fatigue crack propagation direction, ~ 300 µm, is in good accord with the average MnS-inclusion nearest neighbour distance, ~ 310 µm, in this direction. With this information we can also explain the fractographic evidence, Fig. 6, which shows that MnS-inclusion colonies surrounded by hydrogen induced brittle cracks often do not lie in the macroscopic plane of the fatigue crack.

## CONCLUSIONS

The following conclusions can be drawn based on this study.

1. Brittle features in fracture morphology, which are always seen in connection of environmentally influenced cyclic crack growth, are generally associated with the manganese sulfide inclusions; brittle

crack propagation often spreads like a fan from a group of inclusions.

2. Inclusion shape, size and distribution seem to control the extent of brittle fracture and hence the environmental influence.

3. Inclusions localize hydrogen-induced cracking through hydrogen trapping. This type of cracking was observed in front of the main corrosion fatigue crack tip.

4. The treshold of the environmental influence is connected with the plastic zone size exceeding the mean inclusion distance in the fracture plane.

## ACKNOWLEDGEMENTS

This work is a part of the research program on the reliability of nuclear materials performed at the Technical Research Centre of Finland and financed by the Ministry of Trade and Industry of Finland.

## REFERENCES

1. Tomkins, B., 1979, Metal Science 7, 387.

2. Cullen, W.H., Provenzano, V., Törrönen, K.J., Watson, H.E., and Loss, F.J., 1979, "Fatigue Crack Growth of A508 Steel in High-Temperature, Pressurized Reactor Grade Water". NUREG/CR-0969, NRL Memorandum Report 4063, Washington, D.C.

3. Bamford, W.H., and Moon, D.M., 1980, Corrosion 6, 289.

4. Törrönen, K., Hänninen, H., and Cullen, W.H., 1981, Proc. of IAEA Specialists' Meeting on Subcritical Crack Growth, Freiburg, 412.

5. Scott, P.M., and Truswell, A.E., 1981, Proc. of IAEA Specialists' Meeting on Subcritical Crack Growth, Freiburg, 376.

6. Hänninen, H., Törrönen, K., Kemppainen, M., and Salonen, S., 1982, Paper presented at the meeting on Low frequency cyclic loading effects in environmental sensitive fracture, Milan, March 9-11.

7. Jones, R.L., 1981, Proc. of IAEA Specialists' Meeting on Subcritical Crack Growth, Freiburg, 33.

8. Amzallag, C., and Bernard, J.L., 1981, Proc. of IAEA Specialists' Meeting on Subcritical Crack Growth, Freiburg, 412.

9. Bamford, W.H., and Ceschini, L.J., 1980, "Structural Integrity of Water Reactor Pressure Boundary Components", NUREG/CR-1783, NRL Memorandum Report 4500, Washington, D.C.

10. Törrönen, K., and Kemppainen, M., 1981, Proc of ASTM Symposium on Corrosion-Fatigue: Mechanics, Metallurgy, Electrochemistry and Engineering, St. Louis, to be published.

11. Nakai, Y., Kurahashi, H., Emi, T., and Haida, O., 1980, Kawasaki Steel technical report No. 1, (September), 47.

12. Tomkins, B., and Scott, P.M., 1981, Proc. of IAEA Specialists' Meeting on Subcritical Crack Growth, Freiburg, 611.

13. Knott, J.F., 1977, Proc. of the Fourth International Conf. on Fracture, Ed. D.M.R. Taplin, University of Waterloo Press, Canada, 61.

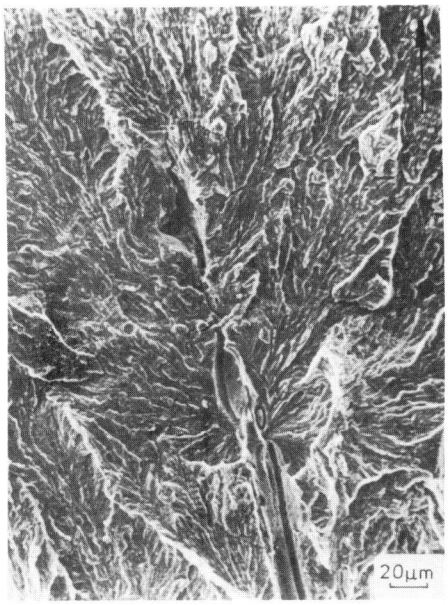


Figure 5 Brittle mode of cracking spreading from MnS inclusion

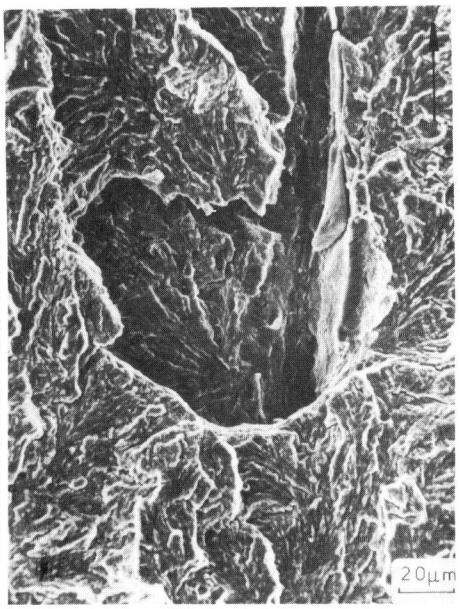


Figure 6 Terraced fracture surface

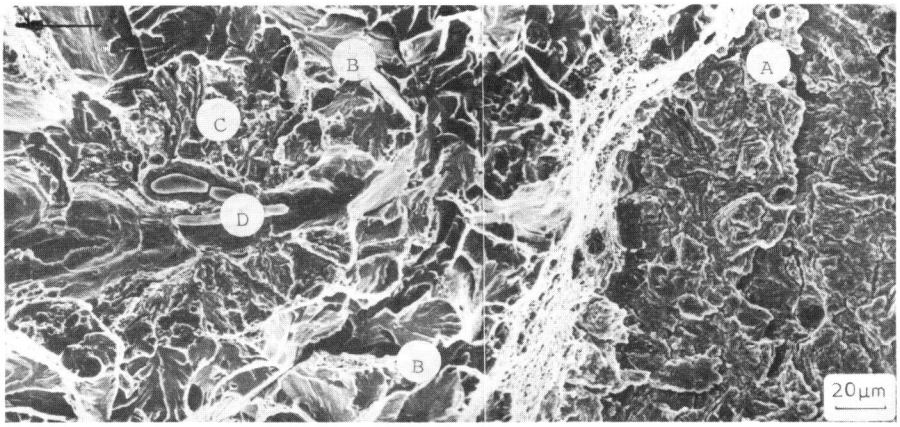


Figure 7 Hydrogen induced microcrack spreading from an inclusion ahead of the main crack tip.

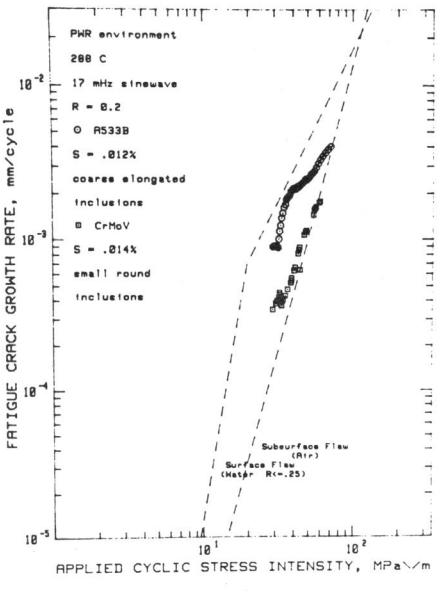


Figure 1 Typical cyclic crack growth results for the two tested steels

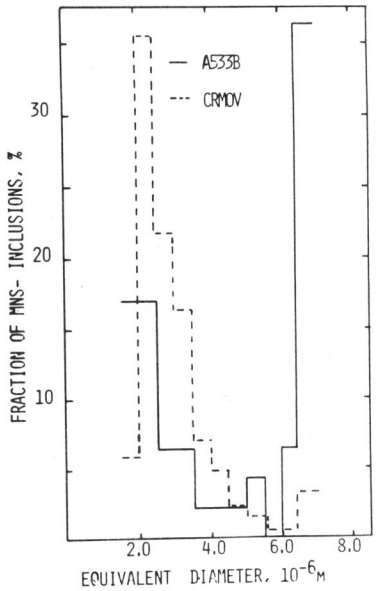


Figure 2 Inclusion size distribution on crack plane for the tested steels

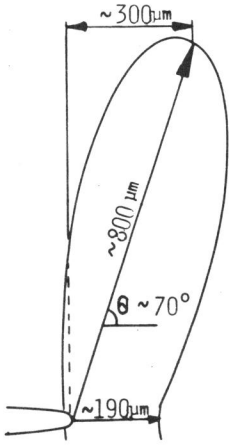


$$R_{MAX}=0.155\bullet(K_{MAX}/\sigma_Y)^2$$

$$R_{MIN}=0.036\bullet(K_{MAX}/\sigma_Y)^2$$

Figure 3 Schematic representation of plastic enclave around crack tip

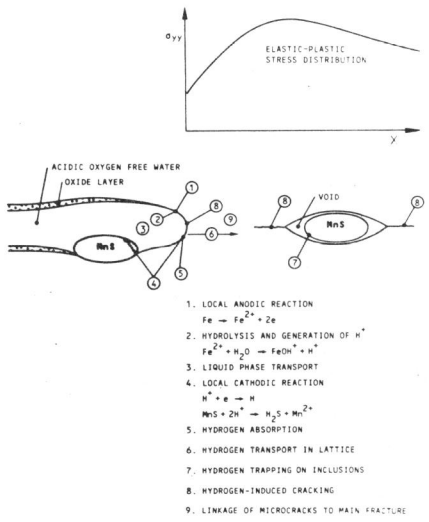


Figure 4 Proposed model for hydrogen induced cracking